Available online at www.sciencedirect.com
ScienceDirect
Trans. Nonferrous Met. Soc. China 30(2020) 1325−1334
Transactions of Nonferrous Metals Society of China
www.tnmsc.cn

Mechanically-induced martensite transformation of NiTiFe shape memory alloy subjected to plane strain compression

Shu-yong JIANG[1], Jun-bo YU[2], Yan-qiu ZHANG[1] , Xiao-dong XING[1]

1. College of Mechanical and Electrical Engineering, Harbin Engineering University, Harbin 150001, China;
2. College of Materials Science and Chemical Engineering, Harbin Engineering University, Harbin 150001, China

Received 9 May 2019; accepted 7 April 2020

Abstract: Based on the channel die compression, NiTiFe shape memory alloy (SMA) was subjected to plane strain compression. Mechanically-induced martensite transformation, nanocrystalline and amorphous phase can be observed in the case of large plastic strain. Mechanically-induced martensite transformation is obviously different from the conventional stress-induced martensite transformation. The former generally occurs after dislocation slip, whereas the latter arises prior to dislocation slip. The occurrence of *B*19' martensite phase contributes to accommodating subsequent plastic deformation of NiTiFe SMA. Mechanically-induced *B*19' martensite is partially stabilized due to the existence of local high stress field and consequently it is unable to be reverted to B2 austenite phase during unloading.
Key words: shape memory alloy; NiTiFe alloy; plastic deformation; martensitic transformation; microstructure

1 Introduction

NiTi shape memory alloy (SMA) possesses two important characteristics, namely shape memory effect and superelasticity, which are related closely to the martensitic transformation induced by temperature change or mechanical stress [1−3]. In order to broaden the engineering application of NiTi SMA, many researchers have added the third element to the binary NiTi SMA for improving the corresponding functional properties. Consequently, the ternary NiTi-based SMAs, including NiTiCu, NiTiNb, NiTiFe, and so on, have been frequently applied in the engineering field [4−7]. In particular, as a ternary NiTi-based SMA, NiTiFe SMA is a superior candidate for manufacturing pipe coupling since it possesses the lower martensite transformation temperature.

Plastic deformation is an indispensable approach in the engineering application of NiTi-based SMAs. On one hand, plastic deformation is used for manufacturing the products of NiTi-based SMAs [8−10]. On the other hand, plastic deformation can improve microstructures and properties of the alloys. In particular, cold plastic deformation can generate plenty of dislocations, and it can result in nanocrystallization and even amorphization of the NiTi-based SMAs. This contributes to enhancing superelasticity, mechanical properties, and biocompatibility, etc. Up to date, many researchers have investigated cold plastic deformation methods of NiTi SMA, including cold drawing [11], cold rolling [12], high pressure torsion [13], local canning compression [14], surface mechanical attrition treatment [15], laser shock peening [16] and ultrasonic nanocrystal surface modification [17]. However, when NiTi SMA with B2 austenite structure is subjected to cold plastic deformation, martensite phase transformation is frequently induced by stress or strain. In fact, stress- or strain-induced martensite

Foundation item: Projects (51475101, 51871070) supported by the National Natural Science Foundation of China
Corresponding author: Xiao-dong XING; Tel: +86-18646332216; E-mail: xingxiaodong@hrbeu.edu.cn
DOI: 10.1016/S1003-6326(20)65299-2

phase transformation is not firstly found in NiTi SMA. For example, OLSON and COHEN [18,19] found that stress- and strain-induced martensitic transformations in 304 stainless steel subjected to plastic deformation, and the occurrence of the former or the latter depends on the specific deformation temperatures. As for the binary NiTi SMAs, stress-induced martensitic transformation has been widely investigated by many researchers [20−24]. In particular, stress-induced martensitic transformation has been observed by means of the corresponding experimental evidence [23,24]. ZHENG et al [25] also found stress-induced martensitic variants in the ternary NiTiNb SMA subjected to the mechanical loading. Strain-induced martensitic transformation is not frequently found in the binary NiTi SMAs. THAKUR et al [26] found strain-induced martensitic transformation in the binary NiTi alloy subjected to shock loading, where a well-defined dislocation substructure is observed, and it should be a typical characteristic of strain-induced martensitic transformation. Few literatures have reported stress-induced or strain-induced martensitic transformations in NiTiFe SMA subjected to plane strain compression.

In the present study, cold plastic deformation of NiTiFe SMA on the basis of plane strain compression is performed. It can be stated that the plane strain compression is obviously different from the aforementioned cold plastic deformation methods of NiTi SMA. For instance, in the case of cold drawing, NiTi SMA is in a two-dimensional compressive stress and a one-dimensional tensile stress state, whereas it is in a three-dimensional strain state, where one-dimensional strain is tensile and two-dimensional strains are compressive [11]. As for cold rolling, NiTi SMA is in a three-dimensional compressive stress state, whereas it is in a three-dimensional strain state, where one-dimensional strain is compressive and two-dimensional strains are tensile [27,28]. High pressure torsion enables NiTi SMA to be in a three-dimensional compressive stress state, whereas it is in a three-dimensional strain state, where one-dimensional strain is compressive and two-dimensional strains are tensile [13]. Stress and strain states of NiTi SMA during local canning compression are similar to the high pressure torsion [29]. Surface mechanical attrition treatment, laser shock peening and ultrasonic nanocrystal surface modification all make NiTi SMA be subjected to surface plastic strain in the case of compressive stress state [15−17]. However, in our work, plane strain compression enables NiTiFe SMA to be in a two-dimensional strain state and in a two-dimensional compressive stress and a one-dimensional tensile stress state. Therefore, the plane strain compression provides a new type of cold plastic deformation for NiTi-based SMAs.

However, no literatures have reported cold plastic deformation of NiTi-based SMAs on the basis of plane strain compression. In the current investigation, cold plastic deformation of NiTiFe SMA was studied via plane strain compression, where mechanically-induced martensite phase transformation was found.

2 Experimental

The as-rolled SMA bar with the composition of $Ni_{47}Ti_{50}Fe_3$ (at.%) was provided by Xi'an Saite Metal Materials Development Co., Ltd, China, and the diameter of it was 9 mm. The NiTiFe samples, which possess the length of 5 mm, the width of 5 mm and the height of 8 mm, were fabricated on the basis of the as-rolled $Ni_{47}Ti_{50}Fe_3$ SMA bar by means of electro-discharge machine (EDM). Then, plane strain compression was imposed on these NiTiFe samples via channel die compression test, as shown in Fig. 1, where X and Y directions represent the length and width directions of NiTiFe sample, respectively, whereas Z direction stands for the height direction of NiTiFe sample. The compression tests were performed on an INSTRON equipment at room temperature, where the strain rate was selected as 0.001 s^{-1}. The heights of the NiTiFe

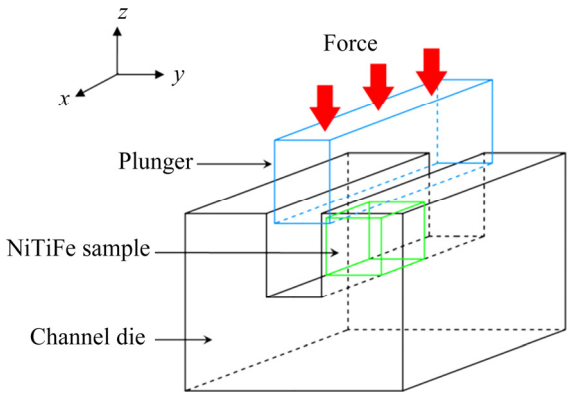

Fig. 1 Schematic diagram for plane strain compression of NiTiFe sample

samples were reduced by 10%, 30% and 60%, respectively.

The microstructure of as-rolled NiTiFe specimens was characterized via electron backscattered diffraction (EBSD). The samples for EBSD were polished by a mechanical method and then were polished by an electrochemical method in a solution comprising 30 vol.% HNO_3 and 70 vol.% CH_3OH at −30 °C. EBSD observation was conducted via a Zeiss ULTRA plus scanning electron microscope (SEM), which possesses Oxford Instruments AZtec combined with EBSD system. During the EBSD analysis, the step size was set as 1.5 μm and the scanning area was determined as 172.5 μm × 231 μm. Figure 2 shows the microstructure of the as-rolled NiTiFe sample, where the average diameter of the grains is 10.61 μm. It can be seen that as-rolled NiTiFe sample is mainly composed of equiaxed grains, which indicates that the as-rolled NiTiFe SMA is subjected to complete recrystallization. In addition, the as-rolled NiTiFe SMA possesses *B*2 austenite phase. Furthermore, differential scanning calorimetry (DSC) experiments were performed and the A_f temperature of the as-rolled NiTiFe SMA was determined as −10.2 °C.

Microstructure of NiTiFe samples subjected to plane strain compression was characterized by transmission electron microscope (TEM). Samples for TEM observation were ground to 70 μm by means of mechanical method. Then, twin-jet thinning was performed in an electrolyte containing 6 vol.% $HClO_4$, 34 vol.% $C4H_{10}O$ and 60 vol.% CH_3OH. TEM experiment was performed on a FEI TECNAI G2 F30 microscope, where the accelerating voltage was set as 300 kV.

3 Results and discussion

Figure 3 indicates the stress−strain curve of NiTiFe sample during plane strain compression. In particular, stress-induced martensite transformation is not observed on the stress−strain curve. It has been reported in Refs. [23,30] that when NiTi sample is composed of *B*2 phase at room temperature, the stress-induced martensite transformation occurs during uniaxial tensile or compressive loading. In other words, the stress−strain curve possesses a stress plateau representing stress-induced martensite transformation. However, in the current investigation, the involved stress plateau is not found on the stress−strain curve of NiTiFe SMA.

For better interpreting the mechanical behaviour of NiTiFe SMA subjected to plane strain compression, the microstructures of NiTiFe sample at various deformation degrees were characterized

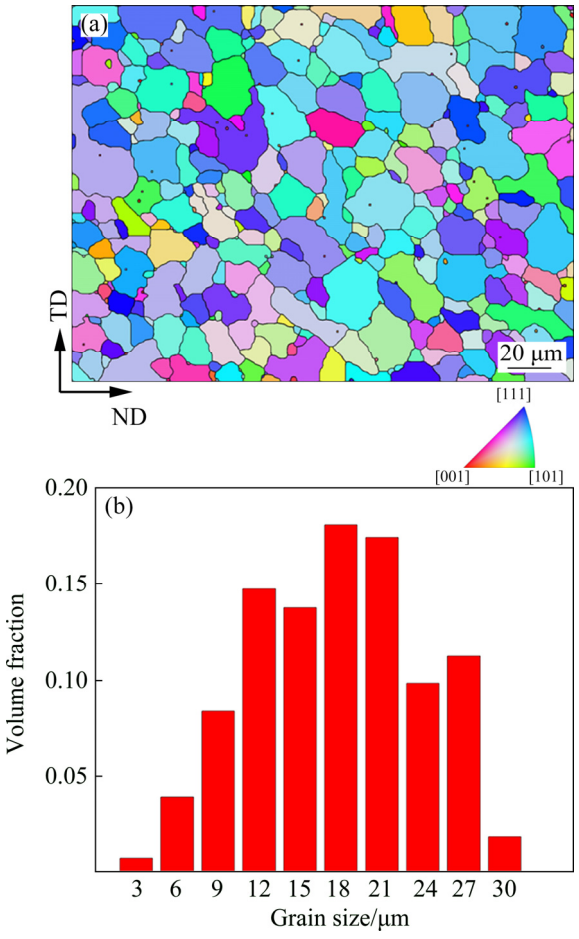

Fig. 2 EBSD microstructure of as-rolled NiTiFe sample (a) and distribution of grain size (b)

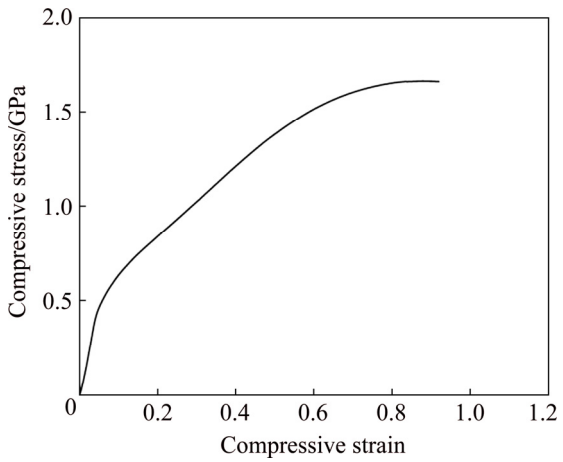

Fig. 3 Stress−strain curve of NiTiFe sample based on plane strain compression

using TEM, as shown in Figs. 4−6. It is noted that inhomogeneous plastic deformation occurs during the compression deformation of NiTiFe sample. *B*19' phase and nanocrystalline are generated at the compressive deformation degree by 10%. With increasing plastic strain, the grains are refined more substantially. When the compressive deformation degree is 30%, *B*19' martensite and nanocrystalline are observed in NiTiFe sample as well. In particular, compared with NiTiFe sample compressed by 10%,

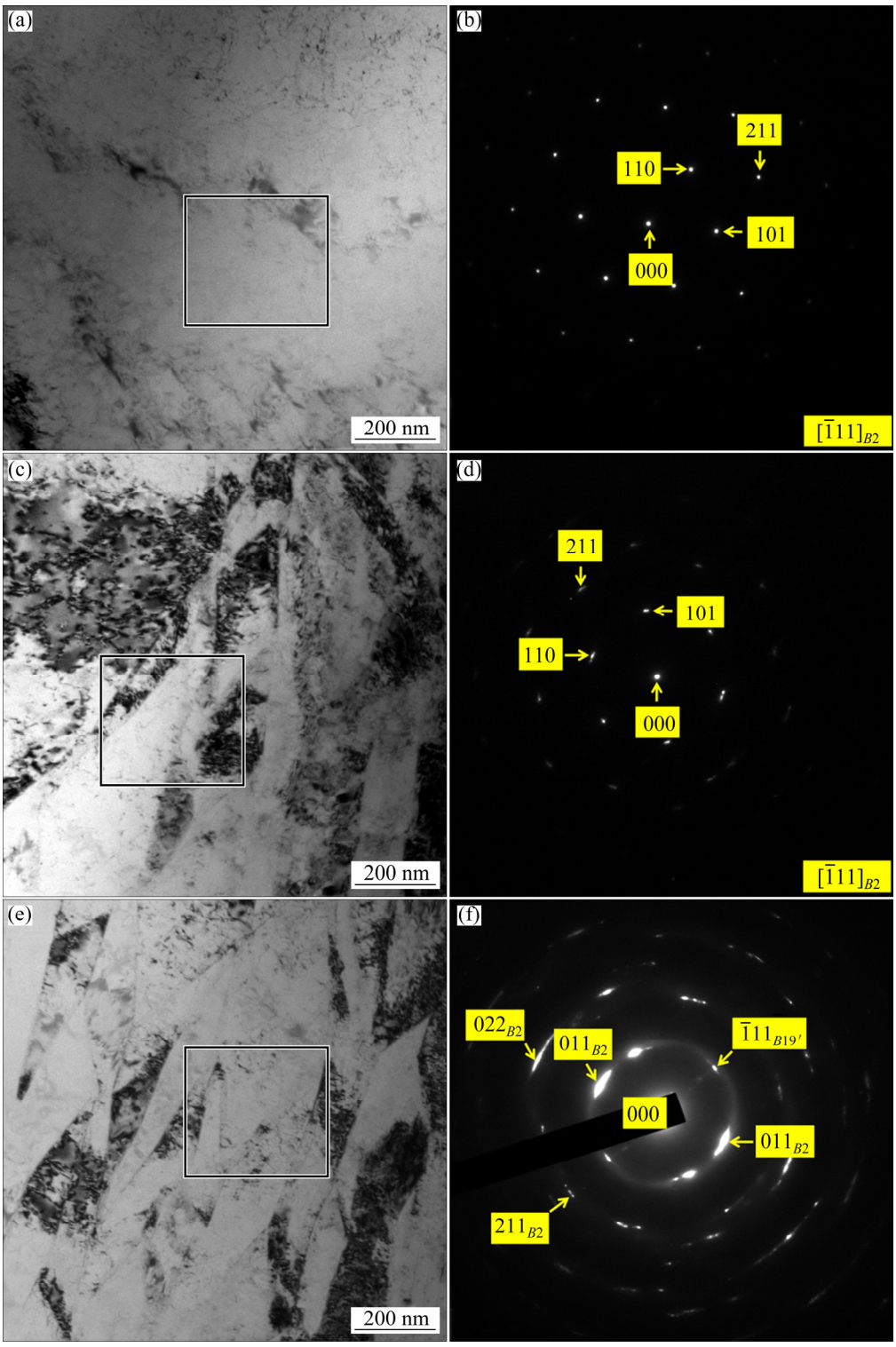

Fig. 4 TEM micrographs of NiTiFe sample compressed by 10% (a, c, e) and corresponding diffraction patterns of selected areas (b, d, f): (a, b) *B*2 phase; (c, d) *B*2 phase and high-density dislocations; (e, f) *B*2 phase, *B*19' phase and nanocrystalline

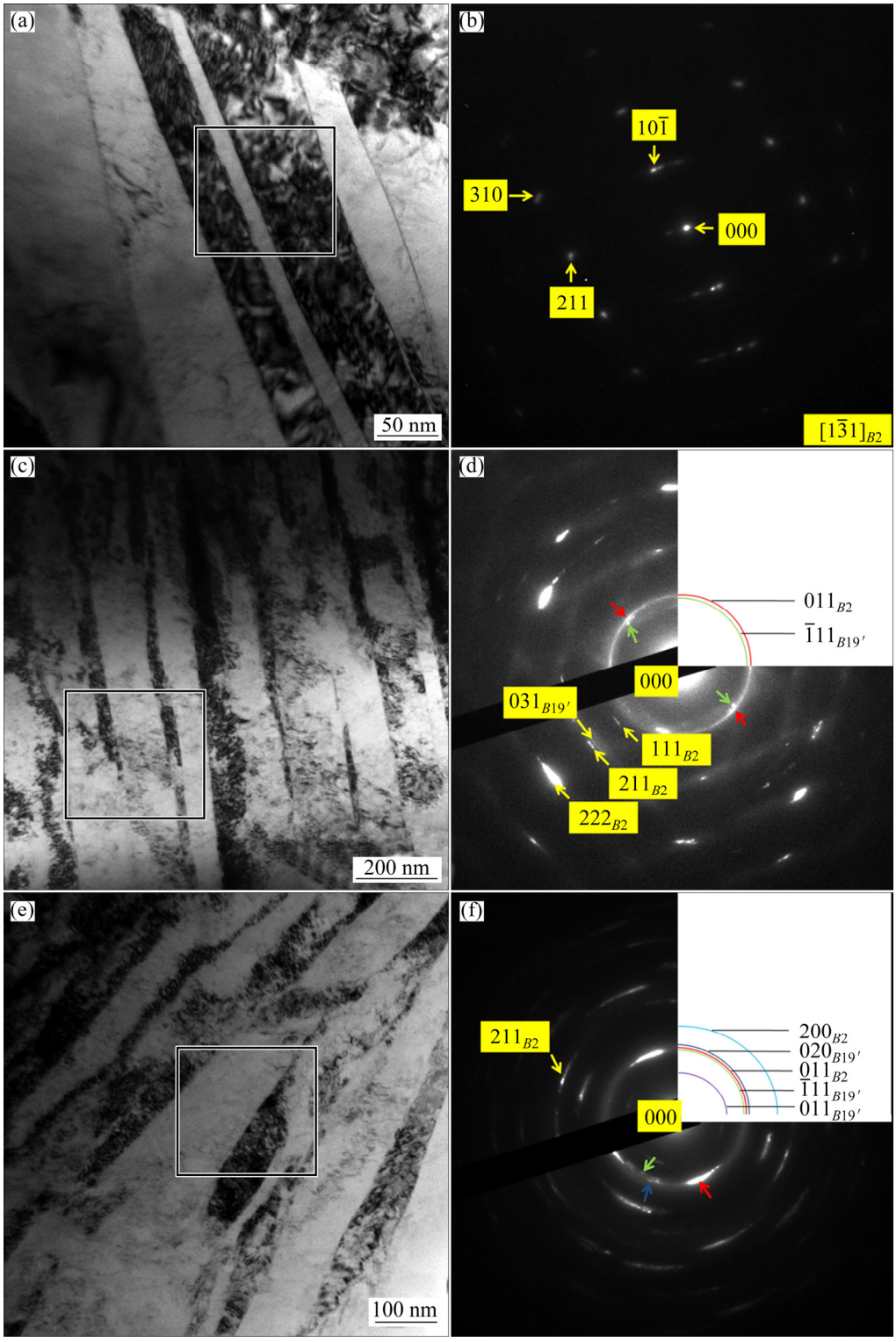

Fig. 5 TEM micrographs of NiTiFe sample compressed by 30% (a, c, e) and corresponding diffraction patterns of selected areas (b, d, f): (a, b) Bright *B*2 phase and high-density dislocations; (c, d) Grain fragment, *B*2 phase and *B*19' phase; (e, f) *B*2 phase, *B*19' phase and nanocrystalline

NiTiFe sample compressed by 30% possesses more obvious martensite lath. When the compressive deformation degree is 60%, amorphous band and amorphous phase can be observed in addition to *B*19' martensite and nanocrystalline.

According to the aforementioned experimental results, it can be deduced that the formation of *B*19' martensite results from mechanically-induced

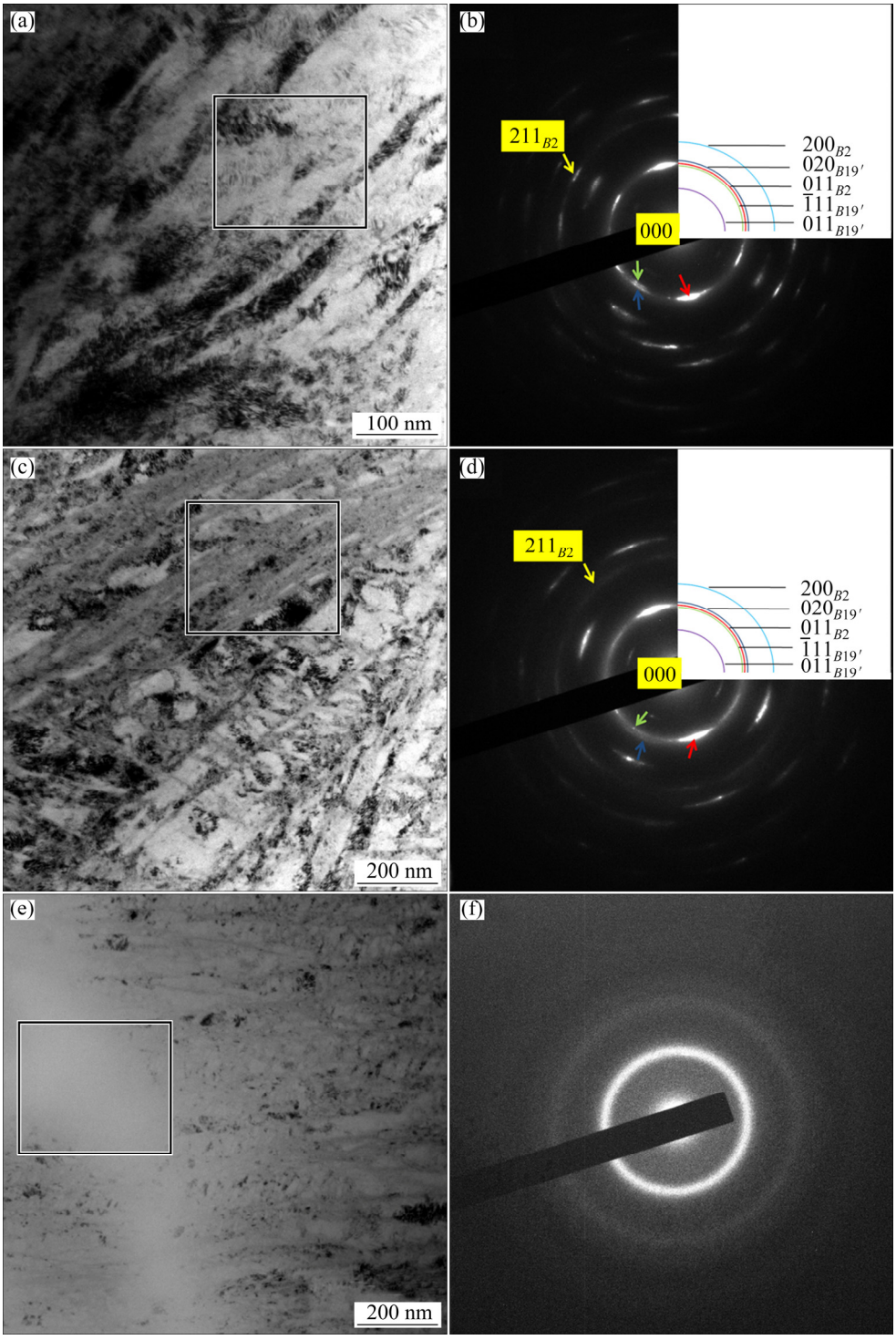

Fig. 6 TEM micrographs of NiTiFe sample compressed by 60% (a, c, e) and corresponding diffraction patterns of selected areas (b, d, f): (a, b) *B*2 phase, *B*19' phase and nanocrystalline; (c, d) *B*2 phase, *B*19' phase, nanocrystalline and amorphous band; (e, f) Dominant amorphous phase

martensitic transformation rather than the conventional stress-induced martensitic transformation only. The mechanically-induced martensitic transformation is attributed to a combination of strain-induced and stress-induced martensitic transformations. In other words, the mechanically-induced martensitic transformation is associated with the initial plastic strain for dislocation slip and subsequent local high stress field. Figure 7 illustrates the mechanism diagram

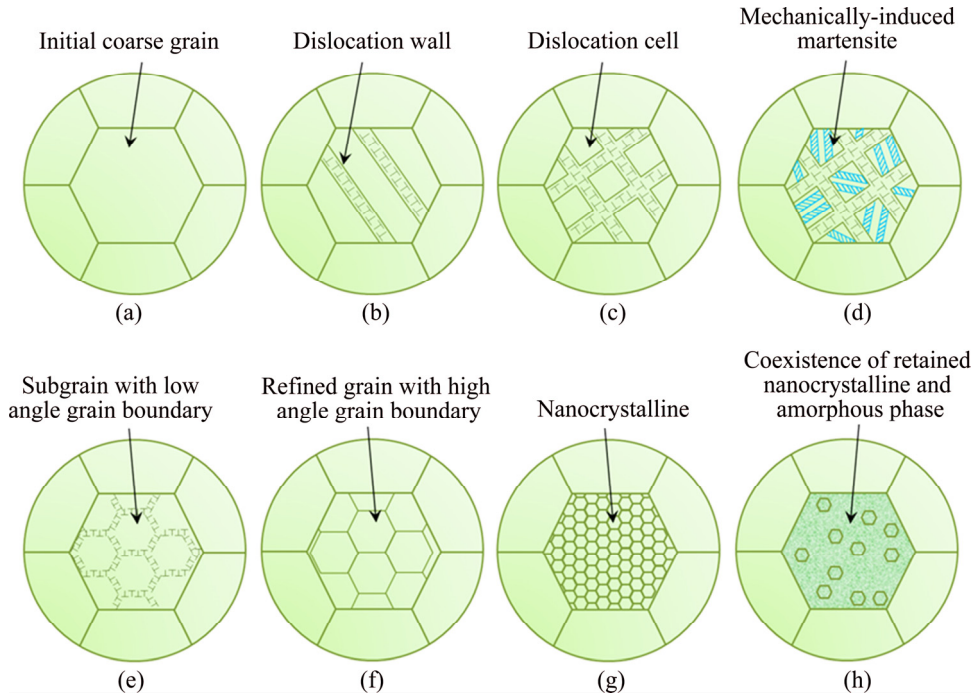

Fig. 7 Mechanism diagram of mechanically-induced martensite, nanocrystallization and amorphization for NiTiFe sample during plane strain compression

for mechanically-induced martensitic transformation, nanocrystallization and amorphization of NiTiFe SMA subjected to the plane strain compression. Firstly, when NiTiFe sample experiences the compression deformation at room temperature, yield stress of dislocation slip is smaller than one that is needed to induce the martensite transformation. As a consequence, stress-induced martensite transformation does not occur prior to the plastic deformation, so slip system can be activated when the external load reaches the critical resolved shear stress (CRSS) for dislocation slip. When the plastic strain is enhanced continuously, the dislocation density increases successively. Therefore, the CRSS for dislocation slip is enhanced with increasing dislocation density. When the CRSS approaches a very high value, the dislocation slip is unable to occur. As a result, the stress that is needed to induce the martensite transformation is smaller than the yield stress for dislocation slip, and thus *B*19' martensite is induced in the case of local high stress field. In addition, the stress-induced martensite transformation appears after plastic deformation for dislocation slip. Furthermore, plastic deformation for dislocation slip is a typical characteristic of strain-induced martensite transformation [17,24]. The occurrence of *B*19' martensite contributes to accommodating subsequent plastic deformation of NiTiFe SMA. The dislocation walls occur with increasing dislocation density. The dislocation walls lay the foundation for the formation of dislocation cells. In addition, the occurrence of mechanically-induced martensite not only changes the crystal structure of NiTiFe SMA, but it alters the crystallographic orientation of NiTiFe SMA as well, which contributes to further plastic deformation of NiTiFe SMA. With the continuous plastic deformation, subgrains with low-angle grain boundaries are generated. Consequently, the low-angle grain boundaries successively absorb the dislocations during plane strain compression and they are turned into the high-angle grain boundaries. This results in the formation of new refined grains. When the grains are repeatedly refined, nanocrystalline can be generated and finally amorphous phase can be induced. Nanocrystalline is considered to be a transition from coarse grain to amorphous phase.

It is well known that stress-induced martensitic transformation frequently appears in NiTi SMA subjected to mechanical loading. However, the stress-induced martensitic transformation is related closely to the chemical composition of NiTi SMA as well as the deformation temperature. If the

deformation temperature is less than A_f temperature and larger than M_s temperature, stress-induced martensite will appear on loading and it will remain stable on unloading. Therefore, subsequent heating is an indispensable procedure in order to make the stress-induced martensite recover to *B*2 phase. The case frequently corresponds to the equiatomic NiTi SMA. If the deformation temperature is larger than A_f temperature and less than M_d temperature, stress-induced martensite will appear on loading, whereas it will be returned to *B*2 phase on unloading. The case usually corresponds to the Ni-rich NiTi SMA. In our work, the A_f temperature of NiTiFe SMA is −10.2 °C and it is obviously lower than room temperature. According to the aforementioned experimental results, in the case of plastic deformation based on the plane strain compression, one portion of mechanically-induced *B*19' martensite will be reverted to *B*2 phase on unloading, whereas another portion of mechanically-induced *B*19' martensite will be stabilized and consequently they will be unable to recover to *B*2 phase.

In summary, mechanically-induced martensite transformation is obviously different from conventional stress-induced martensite transformation. Firstly, the former generally occurs after dislocation slip, whereas the latter arises prior to dislocation slip. Secondly, mechanically-induced martensite transformation is based on large plastic strain, but stress-induced martensite transformation does not need such a large strain. Thirdly, stress-induced *B*19' martensite can be reverted to *B*2 austenite during unloading, whereas mechanically-induced *B*19' martensite is partially stabilized due to the existence of local high stress field. In other words, the stabilized mechanically-induced *B*19' martensite is not returned to *B*2 austenite when the external loading is removed.

4 Conclusions

(1) Plane strain compression results in inhomogeneous plastic deformation of NiTiFe SMA. Mechanically-induced martensite, nanocrystalline and amorphous phase occur when the plastic strain is large enough during plane strain compression.

(2) Plastic deformation for dislocation slip plays a significant role in the formation of mechanically-induced martensite transformation, which is obviously different from conventional stress-induced martensite transformation. Generally, the former occurs after dislocation slip, but the latter arises prior to dislocation slip.

(3) The deformation temperature is larger than the A_f temperature of NiTiFe SMA. The occurrence of mechanically-induced *B*19' martensite phase contributes to accommodating subsequent plastic deformation of NiTiFe SMA. In the case of plastic deformation based on plane strain compression, one portion of mechanically-induced *B*19' martensite will be reverted to *B*2 phase on unloading, whereas another portion of mechanically-induced *B*19' martensite will be stabilized and consequently they will be unable to recover to *B*2 phase.

References

[1] OTSUKA K, REN X. Physical metallurgy of Ti−Ni-based shape memory alloys [J]. Progress in Materials Science, 2005, 50(5): 511−678.

[2] TADAYYON G, MAZINANI M, GUO Y, ZEBARJAD S M, TOFAIL S A M, BIGGS M J P. Study of the microstructure evolution of heat treated Ti-rich NiTi shape memory alloy [J]. Materials Characterization, 2016, 112: 11−19.

[3] HU Li , JIANG Shu-yong, SHI Lai-xin , ZHANG Yan-qiu. Prediction of grain scale plasticity of NiTi shape memory alloy based on crystal plasticity finite element method [J]. Transactions of Nonferrous Metals Society of China, 2019, 29(4): 775−784.

[4] ZHANG Yan-qiu, JIANG Shu-yong, ZHU Xiao-ming, ZHAO Ya-nan, LIANG Yu-long, SUN Dong. Influence of Fe addition on phase transformation behavior of NiTi shape memory alloy [J]. Transactions of Nonferrous Metals Society of China, 2017, 27(7): 1580−1587.

[5] YANG C, CHENG Q R, LIU L H, LI Y H, LI Y Y. Effect of minor Cu content on microstructure and mechanical property of NiTiCu bulk alloys fabricated by crystallization of metallic glass powder [J]. Intermetallics, 2015, 56: 37−43.

[6] SHU X Y, LU S Q, LI G F, LIU J W, PENG P. Nb solution influencing on phase transformation temperature of Ni47Ti44Nb9 alloy [J]. Journal of Alloys and Compounds, 2014, 609: 156−161.

[7] BASU R, MOHTADI-BONAB M A, WANG X, ESKANDARI M, SZPUNAR J A. Role of microstructure on phase transformation behavior in Ni−Ti−Fe shape memory alloys during thermal cycling [J]. Journal of Alloys and Compounds, 2015, 652: 459−469.

[8] DELOBELLE V, CHAGNON G, FAVIER D, ALONSO T. Study of electropulse heat treatment of cold worked NiTi wire: From uniform to localised tensile behaviour [J]. Journal of Materials Processing Technology, 2016, 227:

244−250.

[9] SHARIFI E M, KARIMZADEH F, KERMANPUR A. The effect of cold rolling and annealing on microstructure and tensile properties of the nanostructured Ni50Ti50 shape memory alloy [J]. Materials Science and Engineering A, 2014, 607(3): 33−37.

[10] TADAYYON G, GUO Y, MAZINANI M, ZEBARJAD S M, TIERNAN P, TOFAIL S A M, BIGGS M J P. Effect of different stages of deformation on the microstructure evolution of Ti-rich NiTi shape memory alloy [J]. Materials Characterization, 2017, 125: 51−66.

[11] YU Cun, AOUN B, CUI Li-shan, LIU Yi-nong, YANG Hong, JIANG Xiao-hua, CAI Song, JIANG Da-qiang, LIU Zun-ping, BROWN D. Synchrotron high energy X-ray diffraction study of microstructure evolution of severely cold drawn NiTi wire during annealing [J]. Acta Materialia, 2016, 115: 35−44.

[12] LI Y, LI J Y, LIU M, REN Y Y, CHEN F, YAO G C, MEI Q S. Evolution of microstructure and property of NiTi alloy induced by cold rolling [J]. Journal of Alloys and Compounds, 2015, 653: 156−161.

[13] SHAHMIR H, NILI-AHMADABADI M, HUANG Yi, JUNG J M, KIM H S, LANGDON T G. Shape memory effect in nanocrystalline NiTi alloy processed by high-pressure torsion [J]. Materials Science and Engineering A, 2015, 626: 203−206.

[14] JIANG Shu-yong, HU Li, ZHANG Yan-qiu, LIANG Yu-long. Nanocrystallization and amorphization of NiTi shape memory alloy under severe plastic deformation based on local canning compression [J]. Journal of Non-Crystalline Solids, 2013, 367(1): 23−29.

[15] HU T, CHU C L, WU S L, XU R Z, SUN G Y, HUNG T F, YEUNG K W K, WU Z W, LI G Y, CHU P K. Microstructural evolution in NiTi alloy subjected to surface mechanical attrition treatment and mechanism [J]. Intermetallics, 2011, 19(8): 1136−1145.

[16] WANG Xi, XIA Wei-guang, WU Xian-qiang, WEI Yan-peng, HUANG Chen-guang. Microstructure and mechanical properties of an austenite NiTi shape memory alloy treated with laser induced shock [J]. Materials Science and Engineering A, 2013, 578: 1−5.

[17] CHANG Ye, ZHOU Xian-feng, TELANG A, GAO Hong-yu, REN Zhen-cheng, QIAN Hai-feng, SUSLOV S, GILL A S, MANNAVA S R, QIAN Dong. Surface amorphization of NiTi alloy induced by ultrasonic nanocrystal surface modification for improved mechanical properties [J]. Journal of the Mechanical Behavior of Biomedical Materials, 2016, 53: 455−462.

[18] OLSON G B, COHEN M. Kinetics of strain-induced martensitic nucleation [J]. Metallurgical Transactions A, 1975, 6: 791−795.

[19] OLSON G B, COHEN M. A mechanism for the strain-induced nucleation of martensitic transformations [J]. Journal of the Less-Common Metals, 1972, 28: 107−118.

[20] KARAMAN I, KULKARNI A V, LUO Z P. Transformation behaviour and unusual twinning in a NiTi shape memory alloy ausformed using equal channel angular extrusion [J]. Philosophical Magazine, 2005, 85(16): 1729−1745.

[21] POLATIDIS E, ZOTOV N, MITTEMEIJER E J. Stress-induced phase transformations in thermally cycled superelastic NiTi alloys: In situ X-ray diffraction studies [J]. Powder Diffraction, 2015, 30: 76−82.

[22] TAN G, LIU Y. Comparative study of deformation-induced martensite stabilization via martensite reorientation and stress-induced martensitic transformation in NiTi [J]. Intermetallics, 2004, 12: 373−381.

[23] KATANCHI B, CHOUPANIA N, KHALIL-ALLAFI J, BAGHANI M. Photostress analysis of stress-induced martensite phase transformation in superelastic NiTi [J]. Materials Science and Engineering A, 2017, 688: 202−209.

[24] TIRRY W, SCHRYVERS D. In situ transmission electron microscopy of stress-induced martensite with focus on martensite twinning [J]. Materials Science and Engineering A, 2008, 481−482: 420−425.

[25] ZHENG Y F, CAI W, ZHANG J X, ZHAO L C, YE H Q. Microstructural development inside the stress induced martensite variant in a Ti−Ni−Nb shape memory alloy [J]. Acta Materialia, 2000, 48: 1409−1425.

[26] THAKUR A M, THADHANI N N, SCHWARZ R B. Shock-induced martensitic transformations in near-equiatomic NiTi alloys [J]. Metallurgical and Materials Transactions A, 1997, 28: 1445−1455.

[27] MOHAMMAD SHARIFI E, KERMANPUR A. Superelastic properties of nanocrystalline NiTi shape memory alloy produced by thermomechanical processing [J]. Transactions of Nonferrous Metals Society of China, 2018, 28: 515−523.

[28] MOHAMMAD SHARIFI E, KERMANPUR A. Superelastic behavior of nanostructured $Ti_{50}Ni_{48}Co_2$ shape memory alloy with cold rolling processing [J]. Transactions of Nonferrous Metals Society of China, 2018, 28: 1351−1359.

[29] JIANG Shu-yong, HU Li, ZHAO Ya-nan, ZHANG Yan-qiu, LIANG Yu-long. Plastic yielding of NiTi shape memory alloy under local canning compression [J]. Transactions of Nonferrous Metals Society of China, 2013, 23: 2905−2913.

[30] ELIBOL C, WAGNER F X. Strain rate effects on the localization of the stress-induced martensitic transformation in pseudoelastic NiTi under uniaxial tension, compression and compression–shear [J]. Materials Science and Engineering A, 2015, 643: 194−202.

基于平面应变压缩下的镍钛铁形状记忆合金的机械诱发马氏体相变

江树勇[1]，于俊博[2]，张艳秋[1]，邢晓冬[1]

1. 哈尔滨工程大学 机电工程学院，哈尔滨 150001；
2. 哈尔滨工程大学 材料科学与化学工程学院，哈尔滨 150001

摘　要：基于等通道模具压缩，镍钛铁形状记忆合金经历平面应变压缩变形。通过大塑性变形，可以形成机械诱发马氏体、纳米晶和非晶相。机械诱发马氏体相变明显不同于传统的应力诱发马氏体相变。机械诱发马氏体经常发生在位错滑移之后，而应力诱发马氏体相变发生在位错滑移之前。*B*19'马氏体的出现有助于镍钛铁形状记忆合金后续塑性变形的协调性。局部高应力场的存在导致部分机械诱发 *B*19'马氏体的稳定，因而在卸载条件下，*B*19'马氏体无法逆相转变成 *B*2 奥氏体。

关键词：形状记忆合金；镍钛铁合金；塑性变形；马氏体相变；显微组织

(Edited by Xiang-qun LI)